

## Comparison of simulations to experiment for a detailed analysis of space-charge-limited transient current measurements in organic semiconductors

Marek Z. Szymanski,<sup>1</sup> Irena Kulszewicz-Bajer,<sup>2</sup> Jérôme Faure-Vincent,<sup>1</sup> and David Djurado<sup>1,\*</sup>

<sup>1</sup>INAC, SPram (UMR CNRS-CEA-UJF-5819), CEA Grenoble, 17 rue des Martyrs, 38054 Grenoble, France

<sup>2</sup>Faculty of Chemistry, Warsaw University of Technology, Noakowskiego 3, 00-664 Warsaw, Poland

(Received 23 January 2012; published 10 May 2012)

Space-charge-limited current transients (also referred as time resolved dark injection) is an attractive technique for mobility measurements in low mobility materials, particularly the organic semiconductors. Transients are generally analyzed in terms of the Many-Rakavy theory, which is an approximate analytical solution of the time-dependent drift-diffusion problem after application of a voltage step. In this contribution, we perform full time-dependent drift-diffusion simulation and compare simulated and experimental transients measured on a sample of triaryl-amine based electroactive dendrimer (experimental conditions:  $\mu \approx 10^{-5}$  cm<sup>2</sup>/(Vs),  $L = 300$  nm,  $E < 10^5$  V/cm). We have found that the Many-Rakavy theory is indeed valid for estimating the mobility value, but it fails to predict quantitatively the time-dependent current response. In order to obtain a good agreement in between simulation and experiment, trapping and quasi-ohmic contact models were needed to be taken into account. In the case of the studied electroactive dendrimer, the experimental results were apparently consistent with the constant mobility Many-Rakavy theory, but with this model, a large uncertainty of 20% was found for the mobility value. We show that this uncertainty can be significantly reduced to 10% if a field-dependent mobility is taken into account in the framework of the extended Gaussian disorder model. Finally, we demonstrate that this fitting procedure between simulated and experimental transient responses also permits to unambiguously provide the values of the contact barrier, the trap concentration, the trap depth in addition to that of the mobility of carriers.

DOI: [10.1103/PhysRevB.85.195205](https://doi.org/10.1103/PhysRevB.85.195205)

PACS number(s): 72.80.Le, 72.80.Ng, 73.40.-c, 73.50.-h

### I. INTRODUCTION

Charge carrier mobility is the most crucial property determining the performance and applicability of a semiconducting material. However, more particularly in the field of organic electronics, experimental determination of the charge carrier mobility is still challenging. Time-of-flight (TOF) based technique is certainly one of the preferred mobility determination methods. However, in some cases it might be relatively difficult to be used as it requires relatively thick (several micrometer) samples. Therefore, more commonly, the mobility is deduced from steady state current-voltage characteristics. In such a case, the mobility cannot be determined without an *a priori* knowledge of the contact barrier,<sup>1</sup> even under the assumption of a trap-free material. Such an assumption is most of the time far from being fulfilled in a solution processed material. All these considerations have led us to investigate space-charge-limited current (SCLC) transients in order to estimate the carrier mobility in semiconducting organic solution processed layers. While potentially difficult from an experimental point of view,<sup>2</sup> the technique can in principle permits measurements on thin samples and provide mobility values unaffected by carrier trapping and sample thickness.<sup>3</sup> The obtained current transients are analyzed using the following formula:<sup>4</sup>

$$t_{\max} = 0.786 \frac{L^2}{\mu V}, \quad (1)$$

which relates the time position of the current peak  $t_{\max}$ , the sample thickness  $L$ , the mobility  $\mu$ , and the applied voltage  $V$ . Additional analysis of trapping is also possible<sup>5-8</sup> and, once the mobility is known, the agreement between predicted and obtained steady-state current gives the extent in which the contact

can be considered as ohmic.<sup>9-11</sup> The above formula is approximate (diffusion, initial sample state, and trap release dynamics are neglected) and is known to have a limited validity.<sup>6,12</sup> We would like to show here that a more complete analysis can be achieved by using simulation in parallel to experiments.

Recently there has been a growing interest in performing simulations for interpreting and fitting results of stationary electrical measurements on organic materials. In particular, this approach has permitted the characterization of the contact barrier in a material with known mobility,<sup>13</sup> and the characterization of mobility and disorder from current-voltage characteristics.<sup>14-16</sup> It can be expected that applying this type of analysis to the transient case might permit obtaining even more information. Time-dependent simulation generally takes more time than stationary simulation and is sequential. Also, because the transient responses have a more complex structure than stationary characteristics, the requirements on correctness of the physical model of the sample are more strict than in the time-independent case. It has been recently pointed out that staying on the only basis of standard drift-diffusion theory, used to derive Eq. (1), does not permit us to obtain an agreement between simulated and experimental responses.<sup>17</sup> That directly questions the real accuracy of the mobility estimation using the above formula. Very often the formula has been checked by establishing the good agreement between its results and those obtained with TOF technique.<sup>18</sup> However, it is not always possible to use multiple techniques of mobility measurements to estimate uncertainty of the mobility value and accordingly it is highly desirable to know the mobility uncertainty by employing only the SCLC transient technique.

In this work we develop a method to obtain an experimental-simulation agreement for space-charge-limited transient

responses and an acceptable uncertainty on the mobility value. We use the widely accepted drift-diffusion model, and show which aspects of transport physics must be taken into account to obtain a good agreement with the experimental results.

The organization of the paper is as follows: first, we describe in detail the physical model of transient behavior of a semiconducting sample (Sec. II A); second, the simulation method is developed in Sec. II B, while the exhaustive parameter fitting procedure we used is explained in Sec. II C. The comparison between experimental and simulated current responses, under different model assumptions, is presented in Sec. III. Discussion and conclusions are drawn in Sec. IV.

## II. THEORY AND SIMULATION

### A. Physical model of the sample

As a starting point, let us consider the following system of time-dependent drift-diffusion and trapping equations, which was actually the basis of analytical derivation of formula (1).<sup>4</sup> They describe the time evolution of both the conduction  $n(x, t)$  and trapped  $n_t(x, t)$  charge carrier concentrations and of the electrical potential  $\phi(x, t)$  in an insulator:

$$\frac{d^2\phi}{dx^2} = -\frac{q}{\epsilon_0\epsilon_r}(n + n_t), \quad (2)$$

$$\frac{\partial}{\partial t}(n + n_t) = -\frac{1}{q}\frac{\partial j}{\partial x}, \quad (3)$$

$$j = -q\left(D\frac{\partial n}{\partial x} - \mu n\frac{\partial\phi}{\partial t}\right), \quad (4)$$

$$D = \mu g_3 \frac{kT}{q}, \quad (5)$$

$$\frac{\partial n_t}{\partial t} = r_t n(N_t - n_t) - r_r n_t, \quad (6)$$

where  $q$  is the carrier charge,  $\epsilon_r$  is the relative dielectric permittivity,  $j$  is the carrier current,  $D$  is the diffusion coefficient,  $\mu$  is the charge carrier mobility,  $k$  is the Boltzmann constant,  $T$  is the temperature,  $g_3$  is the so-called diffusion enhancement factor,  $r_t$  and  $r_r$  describe charge trapping and charge releasing rates, and  $N_t$  is the trap concentration. Equation (6) describes the population dynamics of an individual trap. The kinematic coefficients are related to the energetic trap depth  $E_t$  and to the trap cross section  $\sigma_t$  as follows:<sup>19</sup>

$$\frac{r_r}{r_t} = N_0 \exp(-E_t/kT), \quad (7)$$

$$r_t = \langle v\sigma_t \rangle. \quad (8)$$

$N_0 = \frac{1}{a^3}$  is the conduction states density,  $v$  is the charge carrier velocity, and  $\langle \cdot \rangle$  denotes average. In many cases, in the transport model  $\mu = \text{const}$  and  $g_3 = 1$  are assumed. However, it was demonstrated that the model can incorporate the effects of disorder by considering the so-called extended Gaussian disorder, in which  $\mu(T, F, n) = \mu_0 g_1(n, T) g_2(F, T)$  and  $g_3 = g_3(T, n)$ . The functions  $g_1$ ,  $g_2$ ,  $g_3$  are given in Refs. 20–22; they depend on the disorder energy width  $\sigma$  and the intersite distance  $a$ . In this work we will take in consideration both models.

The applied voltage  $V(t)$  is taken into account as a boundary condition for the electrical potential

$$\phi(x = 0, t) = V(t), \quad \phi(x = L, t) = 0. \quad (9)$$

In the case of time-dependent simulation, the displacement current term

$$j_d(x, t) = \epsilon_0\epsilon_r \frac{\partial F}{\partial t} \quad (10)$$

must be included in the calculation of the total current  $j_t$ , which is the current experimentally measured and it follows:

$$j(x, t) + j_d(x, t) = j_t(t). \quad (11)$$

Integrating over the sample length and using the boundary conditions (9), we obtain

$$j_t(t) = \frac{1}{L} \int_0^L j(x, t) dx + \frac{\epsilon_0\epsilon_r}{L} \frac{\partial V}{\partial t}. \quad (12)$$

A crucial problem associated uniquely with simulations of transient currents is the determination of the electrical initial sample state at  $t = 0$ . At the equilibrium, the sample contains charge carriers diffusing into it. In order to be able to solve equilibrium sample state, some established contact models<sup>23,24</sup> expressing current as a function of the electric field  $F$  cannot be used. Indeed, such models by definition predict zero current at the equilibrium, resulting in the so-called empty sample initial condition. Accordingly, a contact theory specifying carrier density at the electrode must be used:<sup>25</sup>

$$n(x = 0) = n_c[F(x = 0)], \quad (13)$$

$$n(x = L) = n_c[-F(x = L)]. \quad (14)$$

The contact interface charge carrier density  $n_c$  is defined in Refs. 22 and 26 and is obtained by establishing the condition of local thermal equilibrium between the metal contact and the organic layer

$$n_c = \int_{-\infty}^{+\infty} \frac{g(E)}{1 + \exp[E/(kT)]} dE, \quad (15)$$

where  $g(E)$  is the density of states in organic layer. For the contact we assume a Gaussian density of states as follows:

$$g(E) = \frac{N_0}{\sqrt{2\pi}\sigma_c a^3} \exp\left[-\frac{(E - \Delta')^2}{2\sigma_c^2}\right], \quad (16)$$

where  $\Delta'$  takes into account the injection barrier ( $\Delta$ ) lowering due to image potential<sup>26,27</sup>

$$\Delta' = \Delta - e\sqrt{\frac{eF}{4\pi\epsilon_0\epsilon_r}}. \quad (17)$$

For consistency we distinguish here contact disorder  $\sigma_c$  from bulk disorder  $\sigma$ . This is because we start by considering the case of constant mobility, for which disorder is irrelevant for bulk transport, but still, contact disorder is necessary to

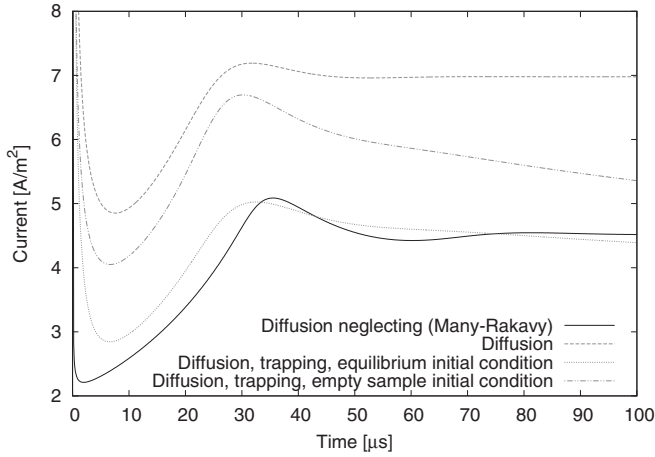


FIG. 1. Simulated dark injection current responses according to different models in which common simulation parameters are sample length  $L = 300$  nm, mobility  $\mu = 10^{-5}$  cm<sup>2</sup>/(Vs), applied voltage 2 V, and relative dielectric permittivity  $\epsilon_r = 3$ . The full line corresponds to the response predicted by the analytical solution. Other lines are obtained by taking into account additional parameters as quoted in the inserted legend and detailed in Sec. II A.

establish the relation between contact charge densities and contact barrier.

In the classical Many Rakavy theory,<sup>4</sup> the above system of equations (2)–(6) is solved for constant mobility, neglecting diffusion, and by assuming empty sample at the beginning of the measurement. Let us now consider the influence of these assumptions when simulating transient responses. Several simulated curves are plotted in Fig. 1. All of them correspond to the same mobility, the same sample thickness, the same voltage, and considering the contact as ohmic. In Fig. 1 the solid curve corresponds to the analytical solution neglecting diffusion while the top curve corresponds to a solution including diffusion, calculated at room temperature. The curves with long time decaying responses correspond to a situation including the presence of traps. They were obtained for the same set of traps, but one assumes equilibrium state at room temperature at time  $t = 0$  while the other one assumes an empty sample. The difference between these two curves directly comes from the existence of pretrapped carriers in the near electrode region, which diffuse from the metal in the equilibrium conditions. The traps are here characterized by the concentration  $N_t = 6.2 \times 10^{15}$  cm<sup>-3</sup>, the trapping coefficient  $r_t = 6.4 \times 10^{-13}$  cm<sup>3</sup>s<sup>-1</sup>, and the release rate  $r_r = 400$  s<sup>-1</sup>. Common simulation parameters are the sample length  $L = 300$  nm, the mobility  $\mu = 10^{-5}$  cm<sup>2</sup>/(Vs), the applied voltage 2 V, the relative dielectric permittivity  $\epsilon_r = 3$ , and charge carrier density at contact plane  $n_c = N_0/2 = 1.22 \times 10^{20}$  cm<sup>-3</sup>.

From Fig. 1 it can be seen that the time position of the peak is, in all cases, close to that predicted by the analytical theory Eq. (1). But it is clear that for a quantitative analysis of the current, neglecting diffusion and assuming empty sample at the beginning of the measurement cause large errors in the evaluation of the current. Accordingly, for comparing experiment and simulation, the sample must be measured in

a well defined (equilibrium) state, and an appropriate contact model must be used in the simulation.

## B. Model implementation

Continuous variables  $\phi$ ,  $n$ ,  $n_t$  are sampled with uniform spatial step  $\Delta x$ . Subscript  $i$  denotes cell index. The potential  $\phi_i$  and the charge concentrations  $n_i$ ,  $n_{t,i}$  are defined inside cells and the current in between cells ( $j_{i+\frac{1}{2}}$  denotes the current flowing from site  $i$  to site  $i + 1$ ). To relate them algebraically we use the Scharfetter-Gummel discretization:<sup>28</sup>

$$j_{i+\frac{1}{2}} = v_{i+\frac{1}{2}} \frac{n_i - e^{-v_{i+\frac{1}{2}} \Delta x / D} n_{i+1}}{1 - e^{-v_{i+\frac{1}{2}} \Delta x / D}}, \quad (18)$$

where charge carrier velocity between cells is

$$v_{i+\frac{1}{2}} = -\mu \frac{\phi_{i+1} - \phi_i}{\Delta}. \quad (19)$$

The formula (18) is obtained by solving  $j = \text{const}$  between cells  $i$  and  $i + 1$  assuming fixed drift velocity  $v$  and diffusion  $D$ . This choice of discretization is optimal for simulation of electrical transport, as it provides exponential interpolation of charge carrier concentration between cells and prevents negative concentration values.

In order to be able to solve the model quickly, we decided to use implicit adaptive time stepping. Indeed, implicit time stepping is convenient as transient responses may change over extended range of time, and explicit time-stepping method would enforce maximum time step for stability even when the solution is close to a stationary state. After discretization of spatial and time derivatives, the differential equations system is converted into the following algebraic equations:

$$\frac{\phi_{i-1} - 2\phi_i + \phi_{i+1}}{\Delta x} + \frac{q}{\epsilon_0 \epsilon_r} (n_i + n_{t,i}) = 0, \quad (20)$$

$$\frac{n_i - n_i^{\text{old}}}{\Delta t} + \frac{n_{t,i} - n_{t,i}^{\text{old}}}{\Delta t} + \frac{1}{q} \frac{j_{i+\frac{1}{2}} - j_{i-\frac{1}{2}}}{\Delta x} = 0, \quad (21)$$

$$\frac{n_{t,i} - n_{t,i}^{\text{old}}}{\Delta t} - r_t n_i (N_t - n_{t,i}) + r_r n_{t,i} = 0. \quad (22)$$

$n_i^{\text{old}}$ ,  $n_{t,i}^{\text{old}}$  refer to conduction and trapped charge concentration, respectively, obtained in the preceding time step. The above nonlinear equations system is solved iteratively using Newton method, once for each time step of duration  $\Delta t$ . For reasons of computation time and numerical precision it is desirable to reduce the number of time steps in the simulation. Due to the character of the time evolution of transient responses, the optimal time-step  $\Delta t$  is much smaller than the transit time ( $\approx t_{\text{max}}$ ) at the beginning of the simulation, and then much longer when the steady state is being approached. Therefore, we implement adaptive time stepping in our simulation. For this purpose we define local error as

$$\epsilon = \left| \frac{j_i(t_0 + \Delta t + \Delta t) - j_i(t_0 + 2\Delta t)}{j_i(t_0 + \Delta t + \Delta t)} \right|, \quad (23)$$

where  $j_i(t_0 + 2\Delta t)$  denotes current value on the basis of a single time step of duration  $2\Delta t$  and  $j_i(t_0 + \Delta t + \Delta t)$  denotes the current value for the same time calculated

with two time steps of duration  $\Delta t$ . During simulation, the time-step duration  $\Delta t$  is automatically adjusted in order to be close to the maximum value for which local error  $\epsilon < \epsilon_{\text{goal}}$ .<sup>29</sup>

For the simulation we used  $\Delta x = 1$  nm and  $\epsilon_{\text{goal}} = 5 \times 10^{-3}$  to define spatial sampling and time stepping, respectively. We checked that use of smaller values do not change significantly the output.

In order to solve equilibrium initial conditions, we run the simulation with zero bias voltage and substituting  $\frac{1}{\Delta t} = 0$ . This gives the solution for the stationary case.

We checked our simulation with results published in Refs. 4, 19, 22, and 26.

### C. Parameters estimation

The transient responses depend in a nonlinear way on the simulation parameters. We decide to assign the same weight to all experimental points, therefore fitting simulation to experimental data consists in finding a set of parameters ( $\mu, \Delta, N_t, r_t, r_r, \dots$ ) for which

$$\chi^2 = \sum_{t,V} [j_t(t,V) - j_{\text{expt}}(t,V)]^2 \quad (24)$$

is minimized.  $j_t$  denotes theoretical current response to voltage  $V$  at time  $t$ , and  $j_{\text{expt}}$  denotes the experimental current. Generally, in order to use efficient local optimization method to obtain parameter values (such as Levenberg-Marquardt), initial estimation of all parameters must be provided, and the final set of values may depend on that estimation. We indeed found that Levenberg-Marquardt method can fail frequently if initially a too large distance between experimental and theoretical points exists.

We therefore propose the following two step procedure for fitting space-charge-limited transients. In a first phase, only trapping parameters are optimized using local search, while mobility and contact barrier are sampled regularly. We perform the process for mobility value estimated from peak positions, and all feasible barrier values sampled regularly with a predefined increment in energy. Once a region of barrier values giving good agreement is found, we take the best set of parameters thus obtained as the starting point and we use the Levenberg-Marquardt algorithm to optimize all the parameters. In order to avoid the risk of finding local minima, we repeat this optimization multiple times with different initial set estimation, obtained by multiplying each parameter in the original set by random numbers close to 1.

The consistency of such a procedure can be justified by considering that in a previous work<sup>19</sup> it was shown that for a given mobility value, the trap concentration and the trap depth (corresponding to the ratio  $r_r/r_t$ ) can be obtained from the shape of the current-voltage curve alone. Furthermore, in Refs. 5 and 6 it was noted that the decay time constant of transient responses defines the trapping rate  $r_t$ . Therefore, fitting for trapping parameters yields an unique solution and fast local search method can be used safely. By contrast, we do not expect it to be always true if fitting with local search methods is done also for contact barrier and mobility.

## III. RESULTS

The sample measured was a layer of a first generation triarylamines based dendrimer  $C_{54}H_{36}N_4(C_4H_9)_6$  similar to that described in Ref. 30, but provided with six peripheral butyl groups for a better solubility. On a clean glass slide was first deposited a bottom golden electrode by evaporation under vacuum. This substrate was then UV treated. A  $0.01$  mmol/cm<sup>3</sup> solution of the dendrimer in THF was then spin coated onto it. Finally, the second golden electrode was also cross evaporated under vacuum on the top of the organic layer. The layer thickness was carefully measured using a profilometer (Ambios-Technology XP-2). Moreover we applied the so-called atomic force microscopy scratch method by using a microscope Nanosurf Mobile S. We obtain a thickness value  $L = 300 \pm 10$  nm. The sample capacitance was checked using Agilent 4294A impedance analyzer and gave  $\epsilon_r \sim 3$ . Transient measurements of hole transport were performed by using the experimental procedure described in Ref. 2. Single measurements duration was 1 s and the delay time between consecutive measurements was 1 s also. The reproducibility of measurements between different fresh samples was checked. All the measurements have been done at room temperature. The responses were measured for voltages from 1.0 to 2.5 V. Because of the high dynamic range of the response signals, the initial part of the responses cannot be measured. Accordingly, we only analyze responses for times longer than  $10 \mu\text{s}$ .

Let us start the analysis by first considering the time position of current response peaks as a function of the applied voltage (Fig. 2). Since obtained responses have less sharp current peaks than predicted by the analytical theory, an objective estimation

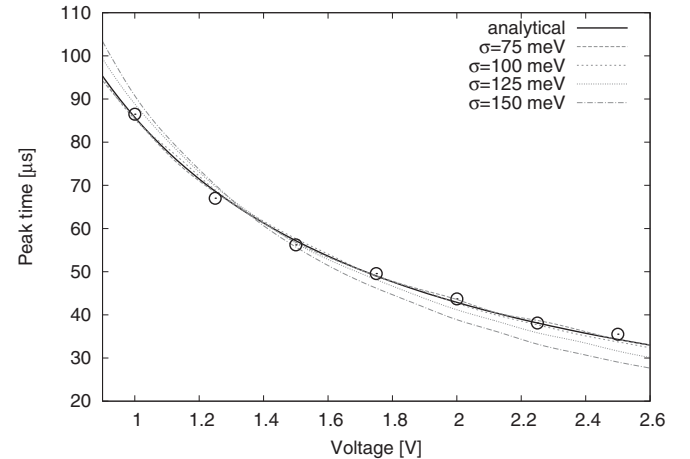


FIG. 2. Experimental peak times as a function of applied voltage. Lines correspond to different fits obtained with analytical model (full line) and models including different degrees of disorder ( $\sigma$ ) (inset legend). The experimental positions are consistent both with analytical model and with extended Gaussian disorder for  $\sigma$  not exceeding approximately 100 meV. Fit to analytical formula (1) gives mobility  $8.25 \times 10^{-6}$  cm<sup>2</sup>/(Vs) (solid curve). Fits to extended Gaussian disorder model with intersite distance  $a = 1.6$  nm and different disorder values  $\sigma = 75, 100, 125, 150$  meV give mobility prefactors  $\mu_0 = 6.32 \times 10^{-6}, 4.53 \times 10^{-6}, 1.99 \times 10^{-6}, 4.25 \times 10^{-7}$  cm<sup>2</sup>/(Vs), respectively. Sample length  $L = 300$  nm.



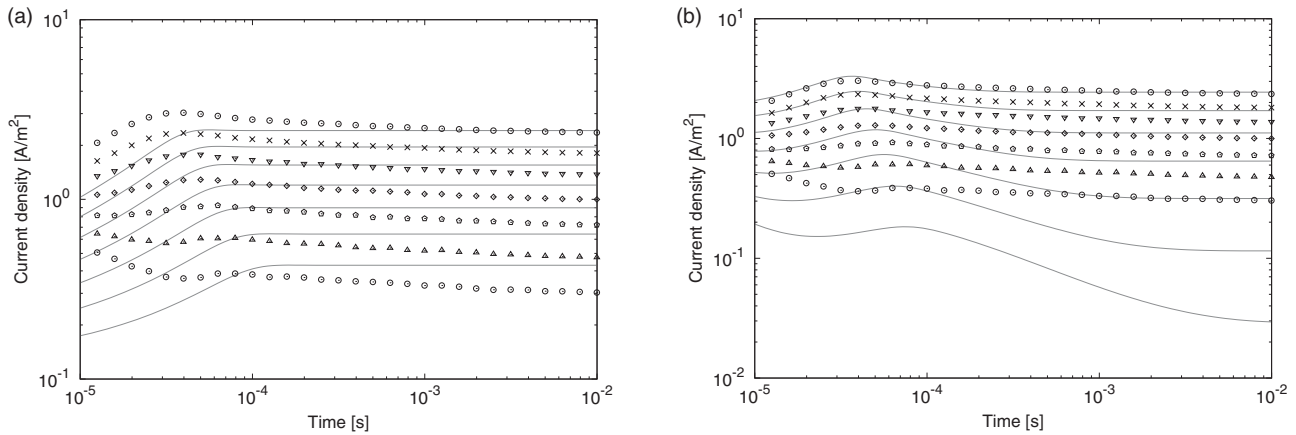


FIG. 3. Experimental transient responses (points) fitted to basic theoretical models (curves): (a) constant mobility and injection barrier;<sup>13</sup> (b) constant mobility with trapping.<sup>19</sup> Common simulation parameters:  $\mu = 8.25 \times 10^{-6} \text{ cm}^2/(\text{Vs})$ ,  $\epsilon_r = 3$ . (a) Injection barrier  $\Delta = 0.456 \text{ eV}$  ( $\sigma_c = 75 \text{ meV}$ ); (b) trap concentration  $N_t = 8.14 \times 10^{15} \text{ cm}^{-3}$ , trapping coefficient  $r_t = 6.856 \times 10^{-12} \text{ cm}^3 \text{ s}^{-1}$ , release rate  $r_r = 12.52$ .

of maximum time is not straightforward. We attempted the maximum time estimation by curve fitting as in Ref. 17. However, we found this procedure to give results strongly dependent on the estimation of the initial location of the peak. Instead, for each response we have calculated the peak time as the average maximum point time obtained for  $n$  ( $n > 1000$ ) realizations of artificial white noise added to the response. The variance of this artificial noise is chosen to be approximately equal to the variance present in the experimental response. The procedure is simple and uses only one parameter (artificial noise variance) for all the responses, in contrast with the curve fitting procedure which is actually semimanual for noisy responses.

Once the peak time positions are known, they can be fitted to formula (1), and the mobility value can be extracted immediately giving  $\mu = 8.25 \times 10^{-6} \text{ cm}^2/(\text{Vs})$ . The experimental responses appear to be in very good agreement with the analytical model suggesting that no field dependent mobility would exist in this sample. Still from Fig. 2 we can also remark that the simulation-experiment agreement stays consistent with bulk disorder values not exceeding approximately 100 meV.

After estimating the mobility, we can realize that the observed current density is smaller than the value which would be theoretically deduced from this mobility value. In order to explain the actual current response, we consider two existing space-charge-limited current lowering mechanisms: contact barrier and trapping (Fig. 3). It turns out that considering each mechanism alone in itself is not sufficient to explain observed current response even qualitatively. The presence of contact barrier alone, considered in Refs. 1 and 13 cannot explain the experimental current transients, at least because it does not reproduce the long term decay following the current peak [Fig. 3(a)]. Therefore, observed current is not purely injection limited. Such decay can be due to traps. In a similar way, the presence of an arbitrary distribution of traps causes a very sharp slope of the current-voltage characteristics over extended range of fields,<sup>19</sup> which is incompatible with our observations. It can be seen that trap distribution compatible with our observation

for highest applied voltage does not account for the low voltages set of the responses [Fig. 3(b)]. However, it is worth to remark that the fit of the contact barrier value gives the superior limit of the barrier height. This is because no mechanism can increase the current and the predicted current is always lower or equal to the observed one.

The impossibility of explaining the current responses by either contact barrier or trapping effect alone, which reduce the current at interface and bulk, respectively, imposes to take into account both effects for the modeling (Fig. 4). We proceeded to find the mobility, trap parameters, and barrier height using the parameter estimation procedure described in Sec. II C. For the initial estimation we used the previously found mobility value  $8.25 \times 10^{-6} \text{ cm}^2/(\text{Vs})$  and we sampled barrier heights every 0.01 eV starting at 0 eV. A satisfactory agreement between simulated and experimental responses has been found only for barrier values around 0.37 eV (assuming  $\sigma_c = 75 \text{ meV}$ ). At this point we then proceeded to the fitting of all other model parameters (including mobility) using previously found values multiplied by a random vector (0.5–1.5) as a starting point. We repeated the process 100 times to obtain a population of possible fits to experimental data. It turned out that solutions with rather different values of mobility describe the data equally well. As seen in Figs. 4(a) and 4(b), smaller mobility values  $\sim 6 \times 10^{-6} \text{ cm}^2/(\text{Vs})$  provide better agreement in the case of lower voltages and higher values  $\sim 8.5 \times 10^{-6} \text{ cm}^2/(\text{Vs})$  in the opposite case. This is reflected by the relatively wide spread of best fit mobility values, as shown in Table I and Fig. 4(c).

We interpret this fact as due to an effect of bulk disorder, which, while not visibly altering peaks positions of the responses, is affecting their shapes significantly. We repeated the search procedure of parameters described above taking into account extended Gaussian disorder model for bulk disorder values  $\sigma = 75 \text{ meV}$  and  $\sigma = 100 \text{ meV}$ . While for  $\sigma = 75 \text{ meV}$  results are similar as those found in the case of constant mobility, for  $\sigma = 100 \text{ meV}$  relative spread of best fit's mobility values is significantly reduced, clearly indicating a better agreement with experimental data as shown in Fig. 5.

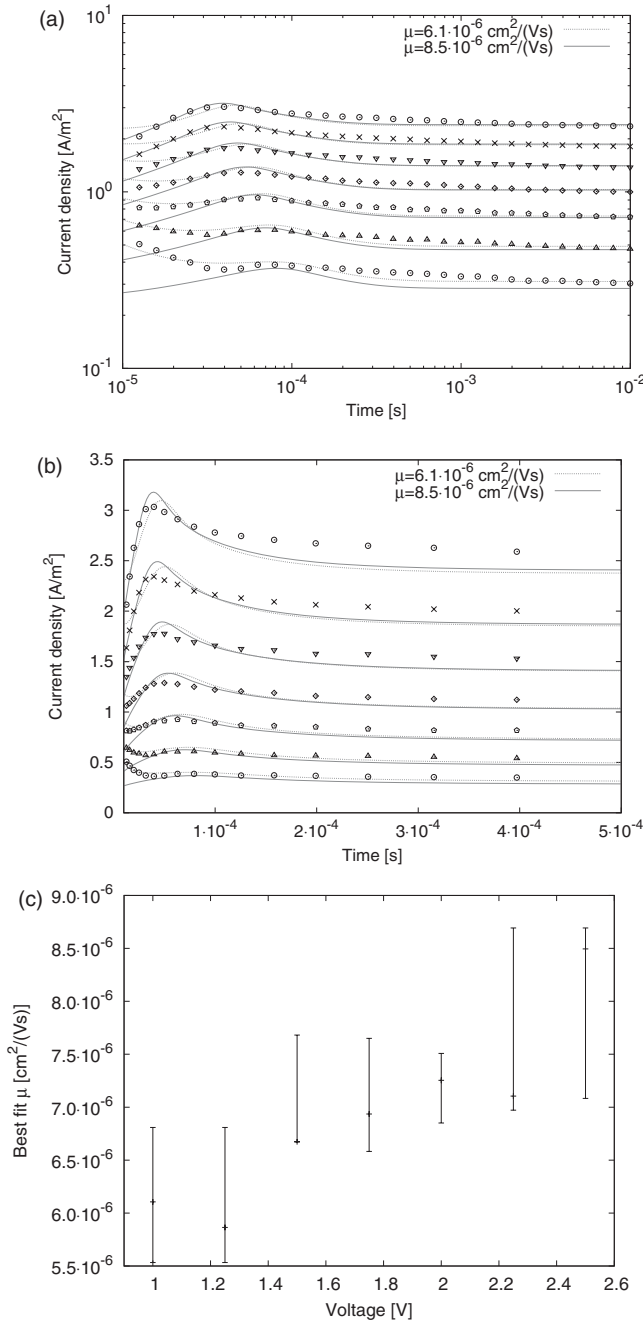


FIG. 4. Experimental transient responses (points) fitted to a model assuming constant mobility and taking into account both interfacial barrier and bulk trapping effects. The same result is presented in logarithmic (a) and linear (b) scale for clarity. For each voltage, best possible goodness of fits is obtained for a range of mobility values (c). Simulation parameters are  $\mu = 6 \times 10^{-6} \text{ cm}^2/(\text{Vs})$ :  $\Delta = 0.283 \text{ eV}$  ( $\sigma_c = 75 \text{ meV}$ ),  $N_t = 7.37 \times 10^{15} \text{ cm}^{-3}$ ,  $r_t = 3.39 \times 10^{-12} \text{ cm}^3 \text{ s}^{-1}$ ,  $r_r = 2820 \text{ s}^{-1}$ ;  $\mu = 8.495 \times 10^{-6} \text{ cm}^2/(\text{Vs})$ :  $\Delta = 0.409 \text{ eV}$ ,  $N_t = 5.09 \times 10^{15} \text{ cm}^{-3}$ ,  $r_t = 3.84 \times 10^{-12} \text{ cm}^3 \text{ s}^{-1}$ ,  $r_r = 3067 \text{ s}^{-1}$ .

Obtained results are summarized in Table I. The dependence of extracted barrier  $\Delta$  on assumed energetic contact disorder  $\sigma_c$  is due to the fact that the charge concentration at contact for a given barrier height strongly depends on the distribution of energy states in the material Eq. (15).<sup>31</sup>

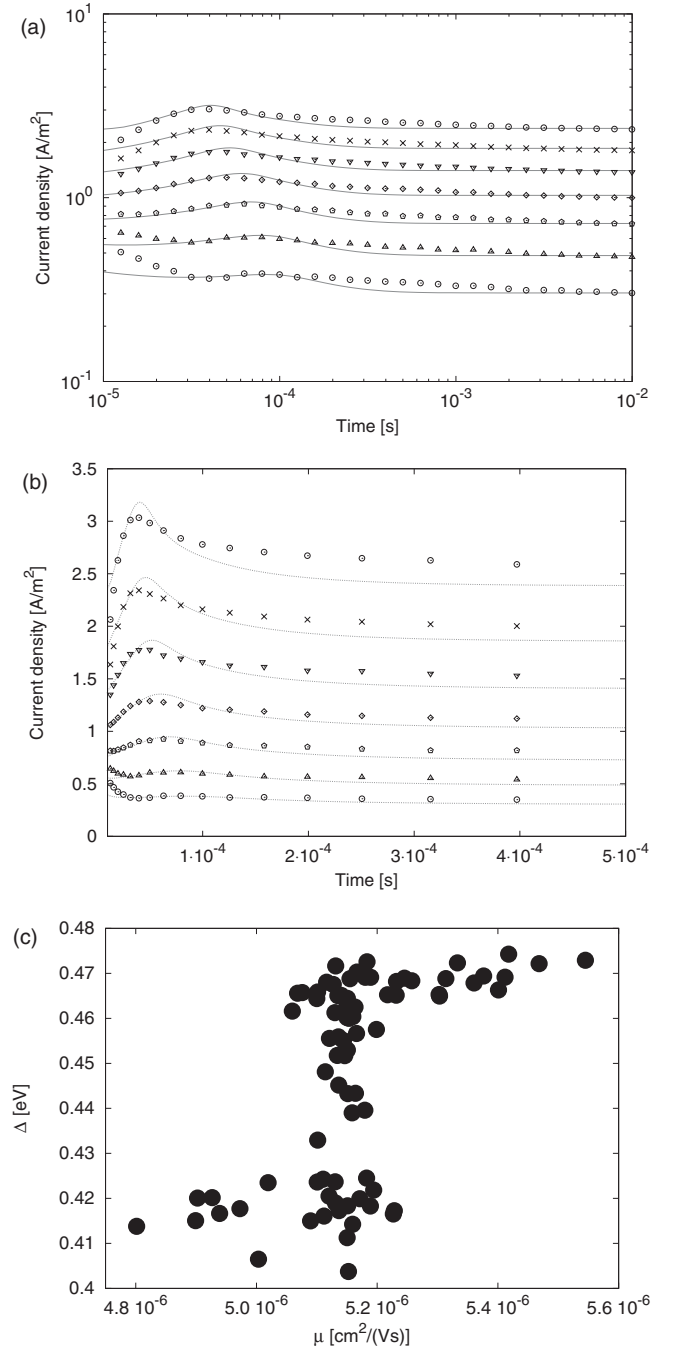


FIG. 5. Results obtained after including the influence of effects of disorder  $\sigma = 100 \text{ meV}$  on diffusion and mobility using extended Gaussian disorder model. (a) and (b) Experimental (points) and simulated (curves) transient responses, in logarithmic and linear scales, respectively. Simulation parameters:  $\sigma = 100 \text{ meV}$ ,  $\mu_0 = 5.02 \times 10^{-6} \text{ cm}^2/(\text{Vs})$ ,  $\Delta = 0.42 \text{ eV}$ ,  $N_t = 6.56 \times 10^{15} \text{ cm}^{-3}$ ,  $r_t = 3.39 \times 10^{-12} \text{ cm}^3 \text{ s}^{-1}$ ,  $r_r = 2998 \text{ s}^{-1}$ . (c) Distribution of best fit's mobility and barrier height values.

#### IV. DISCUSSION AND CONCLUSION

This contribution aimed at first to detail a modeling procedure able to simulate transient current responses obtained in SCLC experiments for estimating the carrier mobility in organic semiconductors. Second, we have shown that comparing simulated and measured time-dependent current

TABLE I. Extracted model parameter values with uncertainties for the two models considered.  $\mu$  denotes charge carrier mobility (in the case of constant mobility model),  $\mu_0$  and  $\sigma$  denote mobility prefactor and bulk disorder (in the case of extended Gaussian disorder model),  $\Delta$  denotes potential barrier,  $\sigma_c$  denotes Gaussian disorder of state energies at metal-organic interface,  $N_t$  denotes trap concentration,  $r_t$  is trapping coefficient,  $r_r$  is release rate,  $E_t$  is calculated trap depth, and  $\sigma_t$  is estimated trapping cross section. Intersite distance is assumed to be  $a = 1.6$  nm, sample length  $L = 300$  nm, relative dielectric constant  $\epsilon_r = 3$ , and temperature  $T = 300$  K.

Model	$\mu = \text{const}$	$\sigma = 100 \text{ meV}$
$\mu$ (cm <sup>2</sup> /Vs)	$(7.1 \pm 1.6) \times 10^{-6}$	–
$\mu_0$ (cm <sup>2</sup> /Vs)	–	$(5.1 \pm 0.4) \times 10^{-6}$
$\Delta$ (eV), $\sigma_c = 50 \text{ meV}$	$0.31 \pm 0.09$	–
$\Delta$ (eV), $\sigma_c = 75 \text{ meV}$	$0.37 \pm 0.09$	–
$\Delta$ (eV), $\sigma_c = 100 \text{ meV}$	$0.44 \pm 0.09$	$0.44 \pm 0.04$
$N_t$ (cm <sup>-3</sup> )	$(6.4 \pm 1.5) \times 10^{15}$	$(6.9 \pm 1) \times 10^{15}$
$r_t$ (cm <sup>3</sup> s <sup>-1</sup> )	$(3.8 \pm 1.4) \times 10^{-12}$	$(2.9 \pm 1.0) \times 10^{-12}$
$r_r$ (s <sup>-1</sup> )	$(3.5 \pm 1.4) \times 10^3$	$(4.3 \pm 1.3) \times 10^3$
$E_t$ (eV)	$(0.32 \pm 0.02)$	$(0.31 \pm 0.02)$
$\sigma_t$ (cm <sup>2</sup> )	$\approx 3 \times 10^{-12}$	$\approx 3 \times 10^{-12}$

responses is a powerful mean to extract not only a relatively accurate value of the mobility (10% of uncertainty) but also important characteristics concerning the contact barrier, the trapping of charge carriers, and the bulk disorder effect.

In particular, we have put emphasis on the definition of the initial electrical state of the sample and we have been led to choose adapted contact model and numerical algorithms which notably differ from those invoked in previous works.<sup>32,33</sup> Moreover, it has been shown how crucial it can be that all the relevant bulk and interfacial effects are included in the theoretical model.

We used a contact model in which are defined conditions of local thermal equilibrium between metal and organic layer.<sup>26</sup>

For solving the resulting time-dependent one-dimensional drift-diffusion system, we use Scharfetter-Gummel discretization method with adaptive implicit time stepping. Resulting nonlinear equation systems are solved using Newton method. This permits fast calculation of current responses without neglecting equilibrium state diffusion of charge carriers into the sample. The resulting simulator is efficient and reliable enough to be used conveniently for fitting space-charge-limited current transient responses.

We compared the results of our simulations assuming equilibrium initial sample state with experimental space-charge-limited current responses obtained with well rested samples. As far as our experimental data are concerned, it was necessary to take into account trapping, contact barrier, and even bulk disorder effects to be able to reproduce correctly

the whole time dependence of the current transient responses (Figs. 3, 4, and 5).

Concerning this last point, we have proved, by developing a relatively simple statistical analysis of results, that including the bulk disorder effects permits to reduce significantly the uncertainty on mobility values from 20% to 10%. This fact seems to us convincing enough to claim that disorder is really an important factor for the interpretation of dark injection transients in this material and this improvement is not due to a simple numerical effect. This conclusion can be drawn in spite of the fact that these measurements have been carried out in a limited range of fields and mostly indicate a behavior with a constant mobility. At the end of this detailed analysis, it is remarkable that the extracted constant mobility value with its uncertainty is still in good agreement with the Many-Rakavy formula (1). It can be noted, however, that the analytical value is slightly higher and this is because the diffusion reduces the prefactor in Eq. (1). This procedure has permitted us to confirm the large influence that the disorder effects can have on transient responses for these materials in agreement with previous work reported in Ref. 12.

However, it is important to stay conscious that in order to obtain a consistent analysis, precautions must be taken to avoid overfitting and to proceed to an exhaustive exploration of parameters space. Especially, we show that care must be taken concerning the influence of initial parameter values on the final fit. The physical correctness of the parameters values depends only on the correctness of the underlying theory. While extended Gaussian disorder model and contact model are well established, it is noteworthy that the kinematics of trapping has not been studied so extensively. In particular, single trap level assumption is probably unrealistic for many samples. Notably, the presence of ionic currents due to impurities or spatial trap distribution would violate our model. Detailed study of universality of the model considered here is a subject for a future work.

With these limitations kept in mind, we have demonstrated that it is possible to model theoretically experimental dark injection responses obtained with such organic semiconducting materials using well established models for electrical transport in insulators. This approach permits a full usability of dark injection mobility measurements; that comes to interestingly moderate some more negative conclusions recently drawn by the authors of Ref. 17, particularly those concerning the sufficiency of existing models for modeling of the transient responses.

## ACKNOWLEDGMENTS

The financial supports of CNRS, CEA (M. Szymanski Ph.D. scholarship), and Région Rhone Alpes are greatly acknowledged. We are also grateful to Jean-Pierre Travers and Jean-François Jacquot for fruitful discussions.

\*Author to whom correspondence must be addressed: david.djurado@cea.fr

<sup>1</sup>Z. B. Wang, M. G. Helander, M. T. Greiner, J. Qiu, and Z. H. Lu, *Phys. Rev. B* **80**, 235325 (2009).

<sup>2</sup>J. C. Scott, S. Ramos, and G. G. Malliaras, *J. Imag. Sci. Technol.* **43**, 233 (1999).

<sup>3</sup>D. Poplavskyy and J. Nelson, *J. Appl. Phys.* **93**, 341 (2003).

<sup>4</sup>A. Many and G. Rakavy, *Phys. Rev.* **126**, 1980 (1962).

- <sup>5</sup>A. Many, S. Z. Weisz, and M. Simhony, *Phys. Rev.* **126**, 1989 (1962).
- <sup>6</sup>M. Simhony and A. Shaulof, *Phys. Rev.* **146**, 598 (1966).
- <sup>7</sup>H. S. Reehal and C. B. Thomas, *J. Phys. D* **10**, 737 (1977).
- <sup>8</sup>K. Eda, *J. Appl. Phys.* **50**, 4436 (1979).
- <sup>9</sup>M. Abkowitz, J. S. Facci, and M. Stolka, *Appl. Phys. Lett.* **63**, 1892 (1993).
- <sup>10</sup>S. C. Tse, S. W. Tsang, and S. K. So, *J. Appl. Phys.* **100**, 063708 (2006).
- <sup>11</sup>Y.-M. Koo, S.-J. Choi, T.-Y. Chu, O.-K. Song, W.-J. Shin, J.-Y. Lee, J. C. Kim, and T.-H. Yoon, *J. Appl. Phys.* **104**, 123707 (2008).
- <sup>12</sup>D. M. Goldie, *J. Phys. D* **32**, 3058 (1999).
- <sup>13</sup>Z. B. Wang, M. G. Helander, M. T. Greiner, J. Qiu, and Z. H. Lu, *J. Appl. Phys.* **107**, 034506 (2010).
- <sup>14</sup>S. L. M. van Mensfoort, S. I. E. Vulto, R. A. J. Janssen, and R. Coehoorn, *Phys. Rev. B* **78**, 085208 (2008).
- <sup>15</sup>R. J. de Vries, S. L. M. van Mensfoort, V. Shabro, S. I. E. Vulto, R. A. J. Janssen, and R. Coehoorn, *Appl. Phys. Lett.* **94**, 163307 (2009).
- <sup>16</sup>J. C. Blakesley, H. S. Clubb, and N. C. Greenham, *Phys. Rev. B* **81**, 045210 (2010).
- <sup>17</sup>T. Esward, S. Knox, H. Jones, P. Brewer, C. Murphy, L. Wright, and J. Williams, *J. Appl. Phys.* **109**, 093707 (2011).
- <sup>18</sup>C. H. Cheung, K. C. Kwok, S. C. Tse, and S. K. So, *J. Appl. Phys.* **103**, 093705 (2008).
- <sup>19</sup>M. A. Lampert and P. Mark, *Current Injection in Solids* (Academic, New York, 1970).
- <sup>20</sup>Y. Roichman and N. Tessler, *Appl. Phys. Lett.* **80**, 1948 (2002).
- <sup>21</sup>W. F. Pasveer, J. Cottaar, C. Tanase, R. Coehoorn, P. A. Bobbert, P. W. M. Blom, D. M. de Leeuw, and M. A. J. Michels, *Phys. Rev. Lett.* **94**, 206601 (2005).
- <sup>22</sup>S. L. M. van Mensfoort and R. Coehoorn, *Phys. Rev. B* **78**, 085207 (2008).
- <sup>23</sup>V. I. Arkhipov, E. V. Emelianova, Y. H. Tak, and H. Bässler, *J. Appl. Phys.* **84**, 848 (1998).
- <sup>24</sup>J. Campbell Scott and G. G. Malliaras, *Chem. Phys. Lett.* **299**, 115 (1999).
- <sup>25</sup>M. A. Lampert and R. B. Schilling, *Phys. Rev. Lett.* **18**, 493 (1967).
- <sup>26</sup>J. J. M. van der Holst, M. A. Uijtewaal, B. Ramachandran, R. Coehoorn, P. A. Bobbert, G. A. de Wijs, and R. A. de Groot, *Phys. Rev. B* **79**, 085203 (2009).
- <sup>27</sup>P. R. Emtage and J. J. O'Dwyer, *Phys. Rev. Lett.* **16**, 356 (1966).
- <sup>28</sup>D. L. Scharfetter and H. K. Gummel, *IEEE Trans. Electron Devices* **16**, 64 (1969).
- <sup>29</sup>K. Gustafsson, M. Lundh, and G. Söderlind, *BIT Numer. Math.* **28**, 287 (1988).
- <sup>30</sup>J. Louie, J. F. Hartwig, and A. J. Fry, *J. Am. Chem. Soc.* **119**, 11695 (1997).
- <sup>31</sup>T. N. Ng, W. R. Silveira, and J. A. Marohn, *Phys. Rev. Lett.* **98**, 066101 (2007).
- <sup>32</sup>J. Staudigel, M. Stößel, F. Steuber, and J. Simmerer, *J. Appl. Phys.* **86**, 3895 (1999).
- <sup>33</sup>B. Ruhstaller, S. A. Carter, S. Barth, H. Riel, W. Riess, and J. C. Scott, *J. Appl. Phys.* **89**, 4575 (2001).